



HAL
open science

Identification of elastic and damping properties of material from a Bayesian formulation of the Force Analysis Technique

Charly Faure, Frédéric Ablitzer, C. Pezerat, Jérôme Antoni

► **To cite this version:**

Charly Faure, Frédéric Ablitzer, C. Pezerat, Jérôme Antoni. Identification of elastic and damping properties of material from a Bayesian formulation of the Force Analysis Technique. ISMA 2016, Sep 2016, LEUVEN, Belgium. hal-01717618

HAL Id: hal-01717618

<https://hal.science/hal-01717618>

Submitted on 26 Feb 2018

HAL is a multi-disciplinary open access archive for the deposit and dissemination of scientific research documents, whether they are published or not. The documents may come from teaching and research institutions in France or abroad, or from public or private research centers.

L'archive ouverte pluridisciplinaire **HAL**, est destinée au dépôt et à la diffusion de documents scientifiques de niveau recherche, publiés ou non, émanant des établissements d'enseignement et de recherche français ou étrangers, des laboratoires publics ou privés.

Identification of elastic and damping properties of material from a Bayesian formulation of the Force Analysis Technique

C. Faure¹, F. Ablitzer¹, C. Pézerat¹, J. Antoni²

¹ Laboratoire d'Acoustique de l'Université du Maine UMR CNRS 6613, Le Mans, France

e-mail: charly.faure@univ-lemans.fr

² Laboratoire Vibrations Acoustique, Univ Lyon, INSA-Lyon, LVA EA677, F-69621, Villeurbanne, France

Abstract

A good knowledge of elastic and damping properties of material is required to predict the dynamic and vibroacoustic behavior of structures, because of their great influence. Recently, an approach derived from the Force Analysis Technique (FAT), initially used to identify external efforts, has been proposed to identify these material properties. The purpose of this work is to present an approach in the same spirit, where the identification of material properties is considered from a Bayesian point of view. The principle of the inverse problem is first exposed in a probabilistic framework where *a priori* and likelihood function are defined precisely. The solving is then performed by using a Monte-Carlo Markov Chain (MCMC) method allowing one to obtain values and uncertainties of results thanks to their probability densities assessments. After the explanation of all steps of the proposed method, some examples are shown, where adjustments are discussed and where elastic and damping material properties are identified on analytically modeled structures.

1 Introduction

Structural models usually serve for both direct and inverse problems, to predict vibration behavior of structures or to infer vibration sources. An error in the model would be propagated as a bias to the identification of sources or displacement fields. The identification of structural parameters is then an important topic in vibroacoustics.

Modal analysis theory based methods are commonly used to infer structural parameter from measurements [1, 2]. However, boundaries conditions must be known, which is not always possible, and structural parameters identification is often performed at natural frequencies of the structure. Another family of methods is based on the identification of the natural wavenumber of the structure, from what structural parameters can be extracted [3–6]. Most of modal based methods limitations are overcome since no boundary condition is required and the analysis can be performed at any frequency.

This work is based on a method called Force Analysis Technique (FAT) initially developed for the identification of vibration sources [7–9] and recently adapted to the structural parameters identification [10]. The principle is to verify the local equation of motion of a structure in an area with no external source. Similarly to the wavenumber based methods, this approach does not required boundary conditions and is applicable at any frequency. The interest to improve the structural identification within the FAT rather than using a wavenumber based method is to perform model and source identifications jointly in the same framework.

In this work, a new regularization strategy is proposed within the Bayesian framework [11] contrary to [10] which is based on the residuals survey. Bayesian methods include Markov Chain Monte Carlo (MCMC) algorithms [12, 13] for the inference of random variables. The Gibbs sampler, a particular case of MCMC

algorithms, is used in this work to perform an automatic and unsupervised regularization, besides the estimation of confidence intervals.

After this introduction, the principle of the FAT based structural parameters identification method is presented in section 2, followed by the adapted Bayesian regularization in section 3. The method is validated on simulation data and results are discussed in section 4, before a conclusion part.

2 Structural parameters identification from FAT

The FAT is based on the equation of motion of a known structure. As an example, the method is presented on a beam within Euler-Bernoulli beam theory. With temporal convention $e^{+j\omega t}$ defined for the angular frequency ω , the harmonic transverse displacement of the beam satisfies Eq. (1),

$$E(1 + j\eta)I \frac{\partial^4 w(x, \omega)}{\partial x^4} - \rho S \omega^2 w(x, \omega) = f(x, \omega), \quad (1)$$

where E is the Young's modulus, $j^2 = \sqrt{-1}$ the imaginary number, η the loss factor, I the moment of inertia, ρ the density, S the section, $w(x, \omega)$ and $f(x, \omega)$ the harmonic transverse displacement and the vibration source distribution at location x and at angular frequency ω , respectively. In an area with no external source applied to the beam, the right hand side of Eq. (1) is equal to zero and the equation of motion can be rewritten as follows

$$\frac{\partial^4 w(x, \omega)}{\partial x^4} = k^4 w(x, \omega), \quad (2)$$

with

$$k = \sqrt[4]{\frac{\rho S \omega^2}{E(1 + j\eta)I}} \quad (3)$$

the natural wavenumber of the beam. Equation 2 means that where there is no external source, the fourth-order partial derivative of the displacement field is proportional to the displacement field itself. Additionally, the multiplicative constant verifying the perfect equality is directly linked to the natural wavenumber of the structure. Considering that the geometry is completely known, as well as the driven frequency and the density, the identification of k leads to the identification of the Young's modulus and the loss factor by

$$E = \Re(k^{-4}) \frac{\rho S \omega^2}{I}, \quad (4)$$

$$\eta = \frac{\Im(k^{-4})}{\Re(k^{-4})}, \quad (5)$$

where $\Re(\bullet)$ stands for the real part and $\Im(\bullet)$ for the imaginary part. To verify experimentally Eq. (2), the displacement field can be obtained directly from measurements while its spatial derivative requires an approximation approach. In this work, the derivative at location x , is estimated by numerical differentiation using the centered finite difference method at first order

$$\frac{\partial^4 w(x_i, \omega)}{\partial x^4} \approx \frac{w(x_{i+2}, \omega) - 4w(x_{i+1}, \omega) + 6w(x_i, \omega) - 4w(x_{i-1}, \omega) + w(x_{i-2}, \omega)}{\Delta_x^4}, \quad (6)$$

where Δ_x is the spacing in the direction x . It can be seen that five displacement points are needed to calculate one spatial derivative point. Shifting the centered stencil $[1; -4; 6; -4; 1]$ of Eq. (6) by one point on a regular mesh grid, most of displacement points can be reused and only one additional displacement point is needed to identify the next derivative point. Following this reasoning and considering a subdomain of the beam (which does not include necessarily its physical boundaries) without any external source, the spatial derivative of the displacement field can be evaluated everywhere except at two points at each boundary of the subdomain. Forward and backward stencils $[3; -14; 16; -24; 11; -2]$ and $[-2; 11; -24; 16; -14; 3]$ respectively) can

then be used at these boundaries. Considering a homogeneous structure, the problem can be expressed in a matrix form

$$\delta_4 \mathbf{w} = k^4 \mathbf{w} \quad (7)$$

where a unique scalar k^4 is sufficient to satisfy the equation, \mathbf{w} is the $(N \times 1)$ vector of displacements and δ_4 is a $(N \times N)$ square matrix build from centered, forward and backward schemes. The natural wavenumber can thus be identified from Eq. (7) by a least-square approach. Taking into account the noise perturbation inherent to experimental measurements, the equation of observation can be written as

$$\mathbf{y} = \mathbf{w} + \mathbf{n} \quad (8)$$

with \mathbf{y} the $(N \times 1)$ vector of observations or noisy displacements and \mathbf{n} the $(N \times 1)$ vector of noise. After replacing the unknown quantity \mathbf{w} by the only one known quantity \mathbf{y} in Eq. (7), the least-square approach is no longer sufficient to identify k because the noise is drastically amplified by the spatial derivative. An appropriate regularization step is then needed.

3 Bayesian formulation of the identification problem

3.1 Bayes theorem

The Tikhonov regularization, commonly used in inverse problem, is not appropriate in this case because it tends to minimize the source norm which is already null by assumption. The Bayesian framework is then particularly suited to the regularization process because it can fit to specificities of each problem by including different kind of *a priori* information.

Bayesian approaches are based on the following theorem to infer the probability of an event from both experiences and *a priori* knowledge,

$$[A | B] \propto [B | A] [A], \quad (9)$$

where \propto means "proportional to". $[A | B]$ is the conditional probability of the event A knowing B , it is called the *a posteriori* probability and refers to the solution of the inference. The conditional probability $[B | A]$ is the likelihood and corresponds to the information extracted from experiences. The quantity $[A]$ stands for the probability density of the random variable A , it is called the *a priori* probability since it encapsulates all theoretical information on A .

3.2 MCMC algorithms

When several variables of the problem are unknown, for example a group of θ_i variables with i from 1 to M , the quantity to infer is then the joint probability denoted $[\theta_1, \theta_2, \dots, \theta_M]$. However, the inference of a multidimensional probability is often intractable analytically and must be performed numerically. Moreover, when the target probability is quite smooth (such as a multivariate Gaussian), it is not necessary to infer the probability everywhere to catch most of the information, a discrete estimation is sufficient. MCMC algorithms are then a powerful tool to perform this discrete inference. A specific feature of these random algorithms is that consecutive samples converge towards the area of maximum of probability. The convergence is then faster than a 'rain-on-the-roof' sampling strategy. The Gibbs sampler, a special case of MCMC algorithms, is used in this work because of its relative simplicity. It consists in sampling consecutively into the conditional probability over each random variable θ_i until the convergence is reached. It can also be seen as a global optimization procedure of a multidimensional cost function.

3.3 *A priori* probability of noise

The perturbation of noise propagates uncertainties to the other problem variables probabilities. It is then important to model the noise probability. Considering an additive white noise, the *a priori* probability of \mathbf{n} is given by

$$[n] \sim \mathcal{N}_c(\mathbf{n}; \mathbf{0}, \sigma_n^2 \mathbf{I}) \quad (10)$$

with a zero mean vector and a scalar variance of noise σ_n^2 . \mathbf{I} stands for the $N \times N$ identity matrix and the N -dimensional multivariate circular complex Gaussian density on \mathbf{x} (see Ref. [14]) with mean vector $\boldsymbol{\mu}$ and covariance matrix $\boldsymbol{\Sigma}$ is defined as

$$\mathcal{N}_c(\mathbf{x}; \boldsymbol{\mu}, \boldsymbol{\Sigma}) = \frac{1}{\pi^N |\boldsymbol{\Sigma}|} \exp\left(-(\mathbf{x} - \boldsymbol{\mu})^H \boldsymbol{\Sigma}^{-1} (\mathbf{x} - \boldsymbol{\mu})\right), \quad (11)$$

where the exponent H stands for the Hermitian transposition. This *a priori* probability of noise

3.4 *A posteriori* probabilities

Three random variables are then totally unknown in this problem and must be inferred to perform the regularization : the noiseless displacement field \mathbf{w} , the wavenumber k and the noise variance σ_n^2 .

3.4.1 Inference of \mathbf{w}

Two information are available for the identification of \mathbf{w} . Firstly, from the equation of observation and the noise distribution (Eqs. (8 ,10)), the probability of the noiseless displacement field is simply expressed by the following relation

$$[\mathbf{w} | \mathbf{y}, \sigma_n^2] \sim \mathcal{N}_c(\mathbf{w}; \mathbf{y}, \sigma_n^2 \mathbf{I}). \quad (12)$$

Secondly, from the equation of motion with no external source (Eq. (2)),

$$[\mathbf{y} | \mathbf{w}, \sigma_n^2, \boldsymbol{\delta}_4] \sim \mathcal{N}_c(\mathbf{y}; k^{-4} \boldsymbol{\delta}_4 \mathbf{w}, \sigma_n^2 \mathbf{I}) \quad (13)$$

Equation (12) can be interpreted as the likelihood since it is always true whatever the structure, while Eq. (13) acts as an *a priori* since it depends on the structure. Both being Gaussian probability (i.e. from the exponential distribution family), their analytical manipulation is easier and the Bayesian theorem yields

$$[\mathbf{w} | \mathbf{y}, \sigma_n^2, \boldsymbol{\delta}_4] \propto [\mathbf{y} | \mathbf{w}, \sigma_n^2, \boldsymbol{\delta}_4] [\mathbf{w} | \mathbf{y}, \sigma_n^2] \quad (14)$$

$$\propto \mathcal{N}_c(\mathbf{w}; \boldsymbol{\mu}_w, \boldsymbol{\Sigma}_w) \quad (15)$$

with :

$$\boldsymbol{\Sigma}_w = \sigma_n^2 \left(\mathbf{I} + \left(k^4 k^{4H} \right)^{-1} \boldsymbol{\delta}_4 \boldsymbol{\delta}_4^H \right)^{-1} \quad (16)$$

$$\boldsymbol{\mu}_w = \left(k^4 k^{4H} \mathbf{I} + \boldsymbol{\delta}_4 \boldsymbol{\delta}_4^H \right)^{-1} \left(k^4 k^{4H} \mathbf{I} + k^4 \boldsymbol{\delta}_4^H \right) \mathbf{y} \quad (17)$$

The maximum of a Gaussian probability corresponds to its mean, so the Maximum *A Posteriori* (MAP), i.e. the most probable value, is given by Eq. (17). The solution of the inference is then directly obtained from $\boldsymbol{\mu}_w$. Two other observations can be made from here. Firstly, the noise variance does not affect the mean of the *a posteriori* probability on \mathbf{w} , it just influences the variance of the estimation from Eq. (16). Secondly, the term applied to \mathbf{y} in Eq. (17) is analogous to a low pass filter whose cutoff frequency is directly linked to the natural wavenumber of the structure k . So the use of a low pass filter depending on the natural wavenumber in Ref. [7] for the source identification seems to be a good intuition.

3.4.2 Inference of k^4

The identification of the Young's modulus and the loss factor from Eqs. (4, 5) is the primary objective before the identification of the wavenumber, so it is preferable to apply the Bayesian theorem directly on k^4 rather than on k . Considering no one *a priori* information, the *a posteriori* probability is directly proportional to the likelihood, from Eqs. (7, 8, 10). Since k^4 is a scalar and $\delta_4 \mathbf{w}$ and \mathbf{y} are both vectors, each point i of the subdomain can be interpreted as a scalar likelihood. The global likelihood is then simply the product of all of them. The Bayesian theorem applied to the inference of k^4 yields

$$[k^4 | \mathbf{w}, \mathbf{y}, \sigma_n^2, \delta_4] \propto [\mathbf{y} | \mathbf{w}, \sigma_n^2, \delta_4] \quad (18)$$

$$\propto \prod_i^N \mathcal{N}_c \left(k^4, \frac{(\delta_4 \mathbf{w})_i}{y_i}, \sigma_n^{-2} \right) \quad (19)$$

$$\propto \mathcal{N}_c (k^4; \mu_{k^4}, \sigma_{k^4}^2) \quad (20)$$

with :

$$\sigma_{k^4}^2 = \frac{\sigma_n^{-2}}{N} \quad (21)$$

$$\mu_{k^4} = \frac{1}{N} \sum_i^N \frac{(\delta_4 \mathbf{w})_i}{y_i} \quad (22)$$

where $(\delta_4 \mathbf{w})_i$ and y_i refer to the i -th element of vectors $\delta_4 \mathbf{w}$ and \mathbf{y} respectively. Here again, the solution of the inference is given by the mean in Eq. (22) and is independent of the noise variance.

3.4.3 Inference of σ_n^2

As \mathbf{y} is known from measurements and \mathbf{w} is inferred from the Bayesian approach, it is possible to identify the noise variance. A variance is always positive and different of zero, a practical choice is to set an inverse-gamma *a priori* probability on σ_n^2 . The inverse-gamma density on x with shape parameter α and scale parameter β is defined as

$$\text{Inv-}\mathcal{G}(x; \alpha, \beta) = \frac{\beta^\alpha}{\Gamma(\alpha)} x^{-\alpha-1} \exp\left(-\frac{\beta}{x}\right) \quad (23)$$

with the gamma function $\Gamma(t) = \int_0^\infty x^{t-1} \exp(-x) dx$. The product of this *a priori* probability and the Gaussian likelihood from the equation of observation (Eq. (8)) yields

$$[\sigma_n^2 | \mathbf{w}, \mathbf{y}] \propto \mathcal{N}_c(\mathbf{y}; \mathbf{w}, \sigma_n^2 \mathbf{I}) \text{Inv-}\mathcal{G}(\sigma_n^2; \alpha_n, \beta_n) \quad (24)$$

$$\propto \text{Inv-}\mathcal{G}(\sigma_n^2; \alpha_n + N, \beta_n + (\mathbf{y} - \mathbf{w})^H (\mathbf{y} - \mathbf{w})) \quad (25)$$

From there, α_n and β_n values can be set so that the *a priori* on the noise variance reflects a particular signal/noise ratio. Another possibility is to fix both parameters to zero. In this case Eq. (25) only depends on the likelihood and no longer on the *a priori*, so the identification of σ_n^2 is totally empirical.

4 Numerical validations

4.1 Synthesis of noisy displacements

To validate numerically this approach, the harmonic transverse displacement field of a simply supported beam excited by a point source is synthesized by using an analytical wave decomposition approach (see Ref. [15])

$$w(x, \omega) = \begin{cases} \frac{A}{2k^3 EI} \left(\sin(kx) \frac{\sin(k(L-x_0))}{\sin(kL)} - \sinh(kx) \frac{\sinh(k(L-x_0))}{\sinh(kL)} \right), & \text{for } x \in [0; x_0] \\ \frac{A}{2k^3 EI} \left(\sin(k(L-x)) \frac{\sin(kx_0)}{\sin(kL)} - \sinh(k(L-x)) \frac{\sinh(kx_0)}{\sinh(kL)} \right), & \text{for } x \in [x_0; L] \end{cases}, \quad (26)$$

where k depends on ω from Eq. 3. All the geometric, structure, source and mesh parameters used for the calculation of k and w from Eqs. (3 , 26) are listed in Tab. 1.

| Length L [m] | Moment of inertia I [m ⁴] | Section S [m ²] |
|--|--|---|
| 1 | $\frac{1}{12} \times 10^{-11}$ | 1×10^{-5} |
| Young's Modulus E [N/m ²] | Structural damping η | Mass density ρ [kg/m ³] |
| 70×10^9 | 4×10^{-2} | 2700 |
| Source frequency ν [Hz] | Source position x_0 [m] | Source amplitude A [N] |
| 280 | 1×10^{-1} | 1 |
| Observation domain x [m] | Number of nodes N | Spatial sampling rate Δ_x [m] |
| [0.3 – 0.8] | 101 | 5×10^{-3} |

Table 1: Geometric, structure, source and mesh characteristics used for the synthesis of the displacement field w .

Following Eq. (8), an additive white noise n is then added to the simulated displacement to mimic measurements as close to reality as possible

$$\mathbf{n} = \frac{(\epsilon' + j\epsilon'')}{\sqrt{2}} \sigma_w 10^{-\frac{\text{SNR}}{20}} \quad (27)$$

with ϵ' and ϵ'' two independent random vectors with the same size as w and sampled from standard complex normal distribution, σ_w the standard deviation of the simulated displacement w and SNR the signal/noise ratio in decibels (dB). The SNR is set to 30 dB in this simulation. Real part of w and y are shown in Fig. 1.

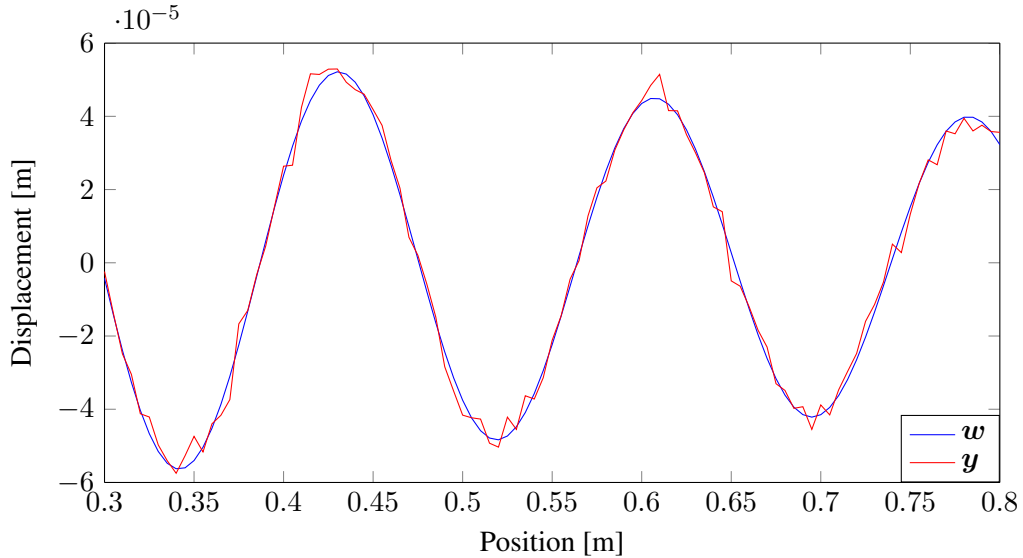


Figure 1: Real part of w and y with SNR = 30 dB.

4.2 Identification of elastic and damping properties

The standard Gibbs sampler consists in sampling consecutively in *a posteriori* probabilities from Eqs. (15 , 20 , 25) until convergence is reached. However, each sample w_{mcmc} from Eq. (15) leads to a displacement

as noisy as \mathbf{y} , even after convergence. Its spatial derivative is quite noisy and the identification of k^4 is as perturbed as with a least-square approach discussed in section 2. It is like if no one regularization was applied. It is then preferable to take some liberties with the standard algorithm and simply identify the MAP from Eq. (17), which corresponds indeed to the filtered \mathbf{y} measurements. The two others variables, k^4 and σ_n^2 , are still sampled from their full *a posteriori* probability, leading to a better exploration of probabilities and to confidence intervals.

The modified Gibbs sampler is initialized with arbitrary values : $\sigma_{n_{initial}}^2 = 1$, $k_{initial}^4 = 10^8$, $\mathbf{w}_{initial} = \mathbf{0}$, while theoretical values are approximately $\sigma_{n_{th}}^2 \approx 1.9 \times 10^{-11}$ and $k_{th}^4 \approx 1.4 \times 10^6 - j5.7 \times 10^4$. The number of iterations is set to 250.

Figures 2 and 3 presents the concatenation of samples, also called a *Markov chain*, of E and η respectively. These results are obtained from the Markov chain of k^4 and from Eqs. (4 , 5). The identification of E is quite close to the theoretical value represented by the horizontal red line : the mean of the converged samples is 70.77×10^9 N/m², namely a relative error of 1.1%. Confidence intervals can also be estimated from the histogram of these converged samples, the centered 90% confidence interval is then in the range of 69.13×10^9 to 72.45×10^9 N/m².

By definition of Eq. (5), $\Im(k^{-4})$ is much lower than $\Re(k^{-4})$. At the same time, the perturbation of $\Im(k^4)$ is of the same order as the one of $\Re(k^4)$ because of the circular Gaussian noise. The estimation of η is then much more dispersed, as seen in Fig. 3. Nonetheless, the mean of the converged samples is 4.01×10^{-2} and the centered 90% confidence interval is in the range of 1.22×10^{-2} to 6.59×10^{-2} . The mean may vary from a simulation to another depending on the number of samples or the snapshot of noise \mathbf{n} , so the mean result may not be as good as it seems. Anyway, several runs of the algorithm allow an estimation of the relative error of 10% approximately. In the same way displacements samples are drawn directly from the MAP, k^4 samples could be drawn from Eq. (22) to increase the mean precision of η , but the information of dispersion given by confidence intervals would be lost.

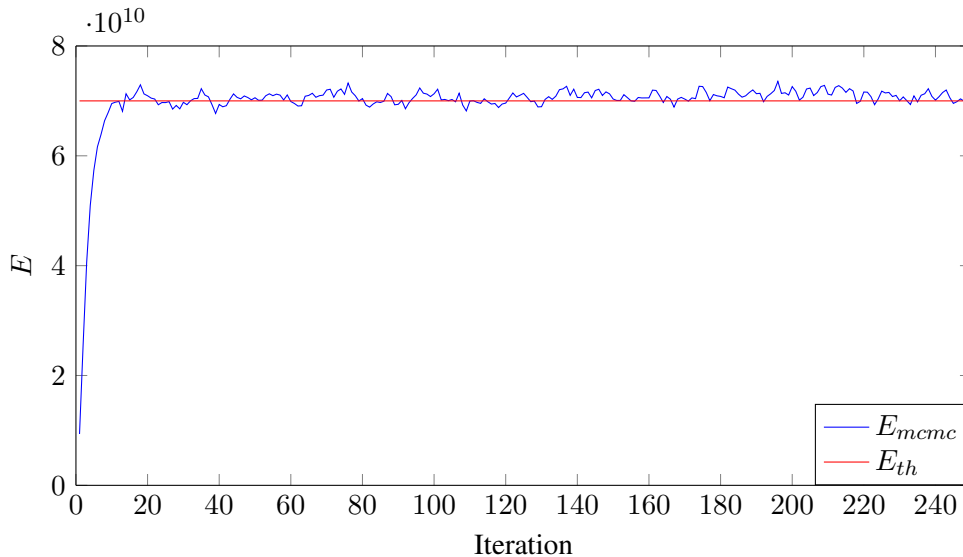


Figure 2: Markov Chain on E , with theoretical value represented by horizontal red line.

The chain of displacements samples is presented in Fig. 4. The variability is solely due to the k^4 chain one since the noise does not appear in Eq. (17). Confidence intervals from these samples would not reflect the complete dispersion of displacements and should not be evaluated.

The mean of the converged displacements samples is presented in Fig. 5 and compared to noisy measurements \mathbf{y} and to the noiseless displacements \mathbf{w} . The result of the MCMC procedure is completely smoothed and closed to \mathbf{w} even if small differences are visible at anti-nodes.

Figure 6 corresponds to the equivalent low pass filter of Eq. (17) applied to measurements \mathbf{y} , calculated with

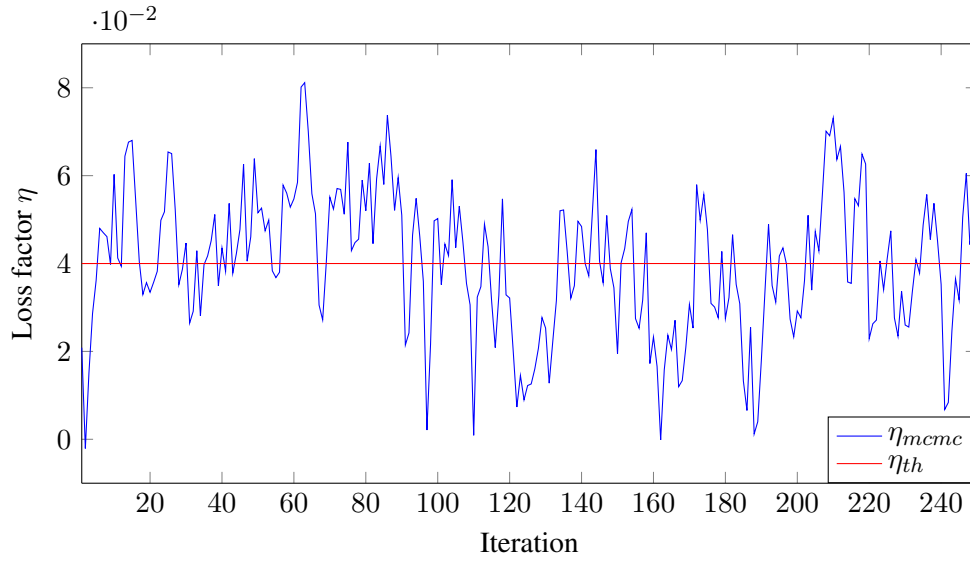


Figure 3: Markov Chain on η , with theoretical value represented by horizontal red line.

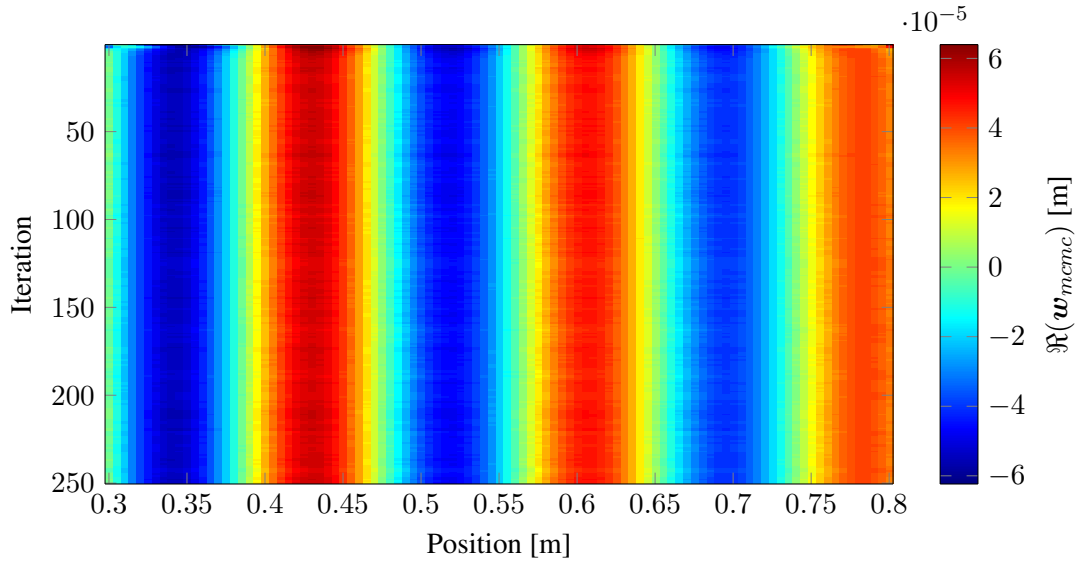


Figure 4: Markov Chain on $\Re(\mathbf{w}_{mcmc})$.

the mean value of the converged k^4 samples. Each line or column represents a typical low pass kernel similar to the sinc function, but it also takes into account the specificity of the differential operator with different stencils at boundaries.

The Markov chain of the noise variance σ_n^2 is finally presented in Fig. 7 on a logarithmic scale. Here again, the identification is quite close to the theoretical variance injected in the simulation. The SNR can be evaluated from the variance of the displacements samples mean and from this noise variance. Considering only the variability of the noise variance to evaluate confidence intervals, the identified SNR is 29.98 dB while the injected SNR is 30 dB, the centered 90% confidence interval is in the range of 29.09 to 30.74 dB.

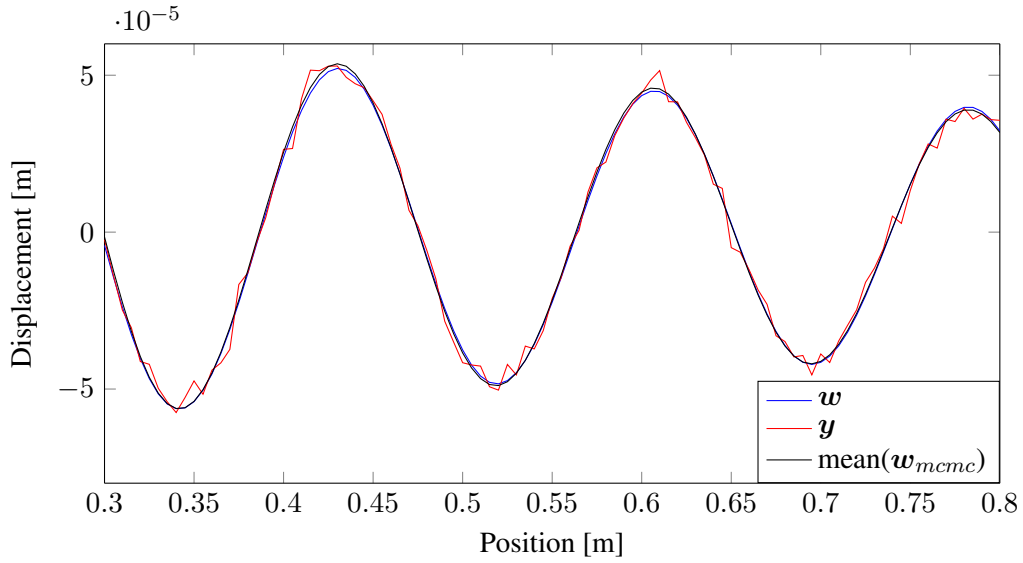


Figure 5: Comparison of w , y and the mean of w_{mcmc} .

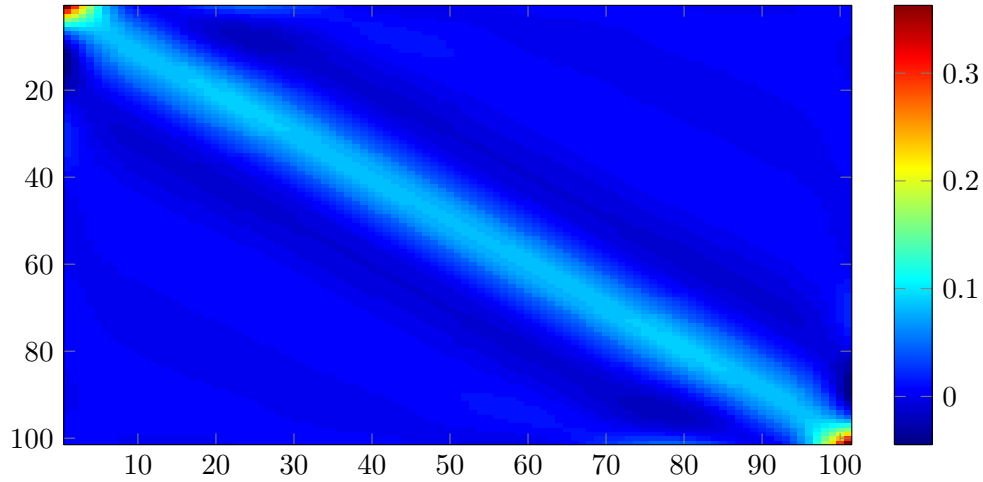


Figure 6: Low pass filter applied to y when convergence is reached.

5 Conclusion

This work is based on Ref. [10] where structural parameters have been inferred from displacement measurements of a structure and two simple assumptions : no external source is applied in the measurements area and the type of structure is known. The use of the Bayesian framework to properly regularize this inverse problem shows some significant improvements. First of all, the procedure is completely unsupervised, it requires only a few parameter initializations which only affects the number of iterations needed to reach convergence. Secondly, the MCMC algorithm allows the propagation of uncertainties and so the identification of confidence intervals. Another interesting point is that the regularization is theoretically independent of the noise variance since the noise influences only precisions of the other random variables but not their modes. Concerning the prospects of the method, the assumption of homogeneous structure may be too restricted, structural parameters can vary spatially in some cases so the method should take it into account. Moreover, this method should be tested on experimental data for a wide frequency range and on different types of structure.

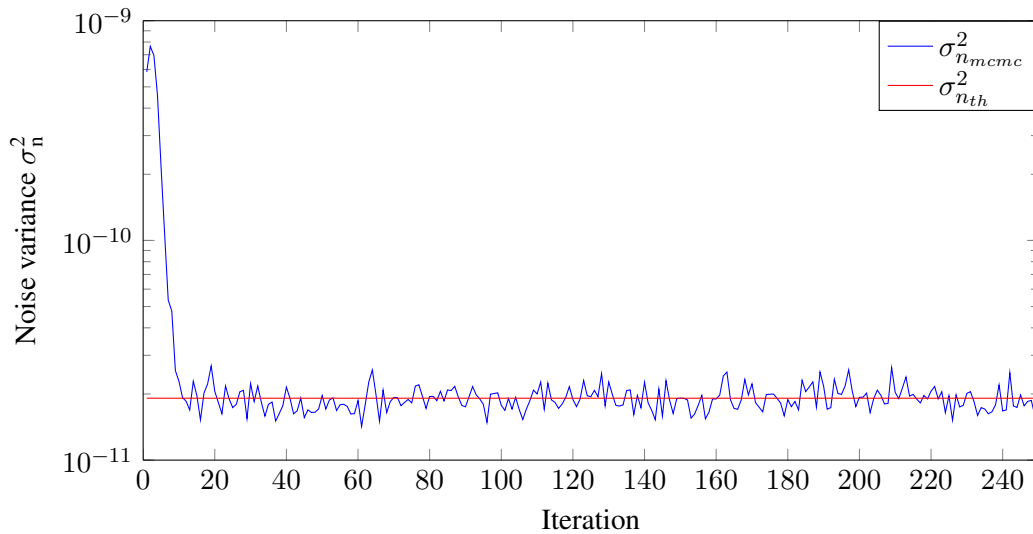


Figure 7: Markov Chain on σ_n^2 , with theoretical value represented by horizontal red line.

Acknowledgements

This work is funded by the TESSA consortium including Vibratex, CEVAA, Pierburg Pump Technology, PSA Peugeot Citroën, Renault, Renault Trucks, Valeo, Sonorhc, CETIM, Centrale-Lyon, INSA-Lyon and Université du Maine.

REFERENCES

- [1] D. J. Ewins, *Modal testing: theory and practice*, Vol. 15, Research studies press Letchworth (1984).
- [2] M. Matter, T. Gmür, J. Cugnoni, A. Schorderet, *Numerical-experimental identification of the elastic and damping properties in composite plates*, *Composite Structures*, Vol. 90, No. 2, (2009), pp. 180–187.
- [3] J. G. McDaniel, W. S. Shepard Jr, *Estimation of structural wave numbers from spatially sparse response measurements*, *The Journal of the Acoustical Society of America*, Vol. 108, No. 4, (2000), pp. 1674–1682.
- [4] J. Berthaut, M. Ichchou, L. Jezequel, *K-space identification of apparent structural behaviour*, *Journal of Sound and Vibration*, Vol. 280, No. 3, (2005), pp. 1125–1131.
- [5] M. Rak, M. Ichchou, J. Holnicki-Szulc, *Identification of structural loss factor from spatially distributed measurements on beams with viscoelastic layer*, *Journal of Sound and Vibration*, Vol. 310, No. 4, (2008), pp. 801–811.
- [6] M. Ichchou, O. Bareille, J. Berthaut, *Identification of effective sandwich structural properties via an inverse wave approach*, *Engineering Structures*, Vol. 30, No. 10, (2008), pp. 2591–2604.
- [7] C. Pezerat, *Méthode d'identification des efforts appliqués sur une structure vibrante, par résolution et régularisation du problème inverse*, Ph.D. thesis, INSA de Lyon (1996).
- [8] M. Djamaa, N. Ouelaa, C. Pezerat, J.-L. Guyader, *Reconstruction of a distributed force applied on a thin cylindrical shell by an inverse method and spatial filtering*, *Journal of sound and vibration*, Vol. 301, No. 3, (2007), pp. 560–575.

- [9] C. Renzi, C. Pezerat, J.-L. Guyader, *Vibratory source identification by using the finite element model of a subdomain of a flexural beam*, Journal of Sound and Vibration, Vol. 332, No. 3, (2013), pp. 545–562.
- [10] F. Ablitzer, C. Pézerat, J.-M. Génevaux, J. Bégué, *Identification of stiffness and damping properties of plates by using the local equation of motion*, Journal of Sound and Vibration, Vol. 333, No. 9, (2014), pp. 2454–2468.
- [11] J.-D. Chazot, E. Zhang, J. Antoni, *Acoustical and mechanical characterization of poroelastic materials using a bayesian approach*, The Journal of the Acoustical Society of America, Vol. 131, No. 6, (2012), pp. 4584–4595.
- [12] S. Brooks, A. Gelman, G. Jones, X.-L. Meng, *Handbook of Markov Chain Monte Carlo*, CRC press (2011).
- [13] G. Casella, E. I. George, *Explaining the gibbs sampler*, The American Statistician, Vol. 46, No. 3, (1992), pp. 167–174.
- [14] J. Rice, *Mathematical statistics and data analysis*, Nelson Education (2006).
- [15] J.-L. Guyader, *Vibration in continuous media*, John Wiley & Sons (2013).